

# Derivation and Fast Computation of Dyadic Green's Functions of Magnetic Vector Potential for Unbounded Uniaxial Anisotropic Media

Jianliang Zhuo<sup>1</sup>, Feng Han<sup>1\*</sup>, Na Liu<sup>1</sup>, Longfang Ye<sup>1</sup>, Hai Liu<sup>1</sup>, and Qing Huo Liu<sup>2</sup>

<sup>1</sup>Institute of Electromagnetics and Acoustics, and Department of Electronic Science  
Xiamen University, Xiamen, Fujian-361008, China  
\*feng.han@xmu.edu.cn

<sup>2</sup>Department of Electrical and Computer Engineering  
Duke University, Durham, NC-27705, USA  
qhliu@duke.edu

**Abstract** — The dyadic Green's function of the magnetic vector-potential  $\mathbf{A}$  (DGFA) for unbounded uniaxial anisotropic media is unavailable in literature but it is needed in numerical computation. The equation of the DGFA was directly derived from the Maxwell's equations. Through the Fourier transform and the inverse Fourier transform, the triple integral form of the DGFA in the spatial domain was obtained. And it was finally simplified to Sommerfeld integrals. In order to verify these formulas, we applied the singularity subtraction technique to evaluate the Sommerfeld integrals rapidly and compared the numerical results with the analytical solutions for degenerated cases for the isotropic unbounded media, as well as the simulated results from a commercial finite element software for uniaxial anisotropic unbounded media. Finally, the effect of the singularity subtraction method was discussed.

**Index Terms** — Dyadic Green's function, magnetic vector-potential, unbounded, uniaxial anisotropic media.

## I. INTRODUCTION

In the past decades, the computation of Green's functions has attracted intensive attention of many researchers. Both the scalar potential [1, 2] and vector potential methods for the computation of Green's functions are suggested. The scalar potential formulations are widely applied to the analysis of complex media [3]. The dyadic Green's functions (DGFs) of the vector potential are the kernel parts of the method of moment (MOM), which is a widely used method in electromagnetic forward and inverse problems [4-11]. So far, the DGFs have been obtained for multilayered isotropic media [12-17], unbounded anisotropic media [18-20], multilayered anisotropic media [21]-24], etc. Michalski and Mosig [17] proposed the transmission line method to calculate the electric- and magnetic-type DGFs in a multilayered medium. Waves were decomposed into transverse electric

(TE) and transverse magnetic (TM) modes in the transmission line analog the multilayered medium, and DGFs were first calculated in the spectral domain and transformed back to the spatial domain later. Electric-type DGFs for general anisotropic media were obtained using the eigenvalue decomposition method by Huang and Lee [20]. The DGFs for the buried sources in stratified anisotropic media were formulated by Ali and Mahoud [24] with both complex tensor permittivities and tensor permeabilities.

However, most of the above research work regarding DGFs focused on the calculation of electric or magnetic fields excited by an infinitesimal electric or magnetic dipole, i.e., the electric- or magnetic-type DGFs. The magnetic vector potential  $\mathbf{A}$  generated by an infinitesimal electric dipole, i.e., the dyadic Green's function  $\overline{\overline{\mathbf{G}}}_{\mathbf{A}\mathbf{J}}$  of the magnetic vector-potential  $\mathbf{A}$  (DGFA), was not frequently studied for anisotropic media. But this auxiliary magnetic vector potential  $\mathbf{A}$  was extensively applied to the solution of antenna radiation problems [25, 26], forward scattering [27, 28] and inverse problems [29]. Fast and precise computation of the DGFA in various media is of great demand because it establishes a direct relation between  $\mathbf{A}$  and the vector current source inside the media. Researchers have proposed some computational methods for the DGFA [17, 30-32]. Moran and Gianzero [31] presented an analytical solution of the DGFA for the uniaxial anisotropic media. It was formulated in the low frequency regime and usually used in well-logging measurements in which the dielectric constant was ignored and no anisotropy of magnetic properties was considered. Abubakar and Habashy [32] provided closed-form tensor Green's functions for an unbounded homogeneous transverse isotropic (TI)-anisotropic medium. In their derivation, the permeability of the media was assumed as a scalar constant instead of the general complex form. Michalski and Mosig [17] derived DGFA from the Green's function of magnetic

field  $\mathbf{H}$  which is derived by transmission line analog method. The mathematical form of the DGFA was not unique and they chose a compact and convenient form.

In this paper, we presented a detailed but mathematically straightforward process for the computation of DGFA in the uniaxial anisotropic medium with both complex tensor permittivity and complex tensor permeability. Based on Maxwell's equations, the spatial domain DGFA in the triple integral was derived through the Fourier transforms and the inverse Fourier transforms. Using eigenvalue methods, Cauchy residue theorem and some mathematical identities, we finally simplified the triple integrals to Sommerfeld integrals. Because of the slow decaying and high oscillating properties, the Sommerfeld integrals can't be computed efficiently by the straightforward numerical integration methods. This process was accelerated by the singularity subtraction method [33] in which a special term was subtracted from each Sommerfeld integrand to make the new integrand rapid decaying, where there is an analytical solution for the integration of each subtracted term. In addition, the singularity of the DGFA when the source point approaching the field point is discussed.

This paper is organized as follows. In Section 2, the DGFA is formulated with both complex tensor permittivity and tensor permeability in unbounded uniaxial anisotropic media. In Section 3, a rapid computation algorithm is applied to the evaluation of Sommerfeld integrals which are deformed from the DGFA. Furthermore, in Section 4, we verify the derived DGFA by comparing them with the analytical solutions in the circumstance of isotropic media, and, with simulated results from a commercial software in the circumstance of uniaxial anisotropic media. And then, we show the efficiency improvements on the convergence of the Sommerfeld integrand by the singularity subtraction method. The summary and conclusions are given in Section 5.

## II. FORMULATIONS AND EQUATIONS

The magnetic vector potential formulation for a homogeneous medium is described in many textbooks. In the absence of magnetic sources (where  $M_i = 0$ ,  $\rho_{mi} = 0$ ), Maxwell's equations (with a time variation of  $e^{j\omega t}$ ) for an unbounded medium are given as:

$$\nabla \times \mathbf{E} = -j\omega \bar{\mu} \mathbf{H}, \quad (1)$$

$$\nabla \times \mathbf{H} = j\omega \bar{\epsilon} \mathbf{E} + \mathbf{J}, \quad (2)$$

$$\nabla \cdot \bar{\epsilon} \mathbf{E} = \rho_e, \quad (3)$$

$$\nabla \cdot \bar{\mu} \mathbf{H} = 0, \quad (4)$$

where  $\mathbf{E}$  is the electric field intensity,  $\mathbf{H}$  is the magnetic field intensity,  $\mathbf{J}$  is the electric current densities,  $\bar{\mu}$  is the complex permeability tensor of the medium, and  $\bar{\epsilon}$  is the complex permittivity tensor, which contains information about the dielectric constant and conductivity tensor of the medium. The complex permittivity  $\bar{\epsilon}$  is defined as

following:

$$\bar{\epsilon} = \bar{\epsilon} + \frac{\bar{\sigma}}{j\omega}, \quad (5)$$

where  $\bar{\epsilon}$  is the real permittivity tensor and  $\bar{\sigma}$  is the conductivity tensor.

In this paper, we assume the optic axis of the uniaxial anisotropic medium is in the  $z$  direction. The permeability, permittivity and conductivity of the medium are written as:

$$\bar{\mu} = \begin{bmatrix} \mu_x & 0 & 0 \\ 0 & \mu_x & 0 \\ 0 & 0 & \mu_z \end{bmatrix}, \quad \bar{\epsilon} = \begin{bmatrix} \epsilon_x & 0 & 0 \\ 0 & \epsilon_x & 0 \\ 0 & 0 & \epsilon_z \end{bmatrix},$$

$$\bar{\sigma} = \begin{bmatrix} \sigma_x & 0 & 0 \\ 0 & \sigma_x & 0 \\ 0 & 0 & \sigma_z \end{bmatrix}. \quad (6)$$

From Equation (4), we can relate the magnetic field and the magnetic vector potential  $\mathbf{A}$  by:

$$\mathbf{H} = \bar{\mu}^{-1} \nabla \times \mathbf{A}. \quad (7)$$

By substituting (7) into (1) and using the vector identity that the curl of the gradient of any scalar function is zero, we can write the electric field as:

$$\mathbf{E} = -j\omega \mathbf{A} - \nabla \phi_e, \quad (8)$$

where  $\phi_e$  is a scalar electric potential.

By substituting (7) and (8) into (2), we obtain the equation of the magnetic vector potential  $\mathbf{A}$  and the scalar potential  $\phi_e$  as:

$$\nabla \times \bar{\mu}^{-1} \nabla \times \mathbf{A} - \omega^2 \bar{\epsilon} \mathbf{A} + j\omega \bar{\epsilon} (\nabla \phi_e) = \mathbf{J}. \quad (9)$$

For anisotropic media, we use the gauge by Chew [34]:

$$\nabla \cdot \bar{\epsilon} \mathbf{A} + \chi j\omega \phi_e = 0, \quad (10)$$

where  $\chi$  is an arbitrary function of position  $\bar{\mathbf{r}}$ , and  $\chi = \alpha [\bar{\epsilon} \cdot \bar{\mu} \cdot \bar{\epsilon}]$ . Note that  $\alpha$  can be chosen arbitrarily. For different selection, the DGFA will be different. But the electric and magnetic field computed using DGFA will not change. In order to simplify the subsequent mathematical derivations and numerical calculation, we choose  $\alpha = \frac{1}{\epsilon_x^4 \mu_x^2}$ , where  $\epsilon_x = \epsilon_x + \frac{\sigma_x}{j\omega}$ . And then,

$$\chi = \mu_z \epsilon_z^2, \quad (11)$$

where  $\epsilon_z = \epsilon_z + \frac{\sigma_z}{j\omega}$ . For this value of  $\chi$ , the gauge in (10) will degenerate into the Lorentz gauge if the medium is isotropic.

Substituting (10) and (11) into (9), we obtain the equation of magnetic vector potential  $\mathbf{A}$  as:

$$\nabla \times \bar{\mu}^{-1} \nabla \times \mathbf{A} - \omega^2 \bar{\epsilon} \mathbf{A} + \frac{1}{\mu_z \epsilon_z^2} \bar{\epsilon} \nabla (\nabla \phi_e) = \mathbf{J}. \quad (12)$$

Our choice of  $\alpha = \frac{1}{\epsilon_x^4 \mu_x^2}$  guarantees that the three terms in the left side of Equation (12) have the same order of coefficient magnitude. And Equation (12) can be expressed in a more compact form as:

$$\bar{Z}_E \mathbf{A} = \mathbf{J}, \quad (13)$$

where  $\bar{Z}_E$  is a second order differential matrix, and its detailed expression is shown in the Appendix A.

If the current source is a unit point source, Equation (13) becomes the equation of the DGFA  $\bar{G}_{AJ}(\bar{\mathbf{r}}, \bar{\mathbf{r}}')$  in

the spatial domain as following:

$$\bar{\bar{Z}}_E \bar{\bar{G}}_{AJ}(\bar{\mathbf{r}}, \bar{\mathbf{r}}') = \delta(\bar{\mathbf{r}}, \bar{\mathbf{r}}') \bar{\mathbf{I}}, \quad (14)$$

where  $\bar{\mathbf{I}}$  is the unit dyadic, and the unitary point source excitation is located at  $\bar{\mathbf{r}}' = \hat{\mathbf{x}}x' + \hat{\mathbf{y}}y' + \hat{\mathbf{z}}z'$ .

By applying the spatial Fourier transform to (14), we obtain the equation of DGFA  $\bar{\bar{G}}_{AJ}(\bar{\mathbf{k}}, \bar{\mathbf{r}}')$  in the spectral domain as following:

$$\bar{\bar{Z}}_A \bar{\bar{G}}_{AJ}(\bar{\mathbf{k}}, \bar{\mathbf{r}}') = e^{j\bar{\mathbf{k}} \cdot \bar{\mathbf{r}}'} \bar{\mathbf{I}}, \quad (15)$$

where  $\bar{\mathbf{k}}$  is the wave vector, which is given as  $\bar{\mathbf{r}}' = \hat{\mathbf{x}}k_x + \hat{\mathbf{y}}k_y + \hat{\mathbf{z}}k_z$ , and  $\bar{\bar{Z}}_A$  is the electric wave matrix about  $(k_x, k_y, k_z)$ , whose complete expression is shown in the Appendix B.

Equation (15) can be rewritten as:

$$\bar{\bar{G}}_{AJ}(\bar{\mathbf{k}}, \bar{\mathbf{r}}') = \frac{\bar{\bar{Z}}_A}{|\bar{\bar{Z}}_A|} e^{j\bar{\mathbf{k}} \cdot \bar{\mathbf{r}}'}, \quad (16)$$

where  $\bar{\bar{Z}}_A^a$  is the adjoint matrix of  $\bar{\bar{Z}}_A$ , whose determinant is  $|\bar{\bar{Z}}_A|$ .

Applying the spatial inverse Fourier transform, we obtain the relationship between the spatial domain DGFA  $\bar{\bar{G}}_{AJ}(\bar{\mathbf{r}}, \bar{\mathbf{r}}')$  and the spectral domain DGFA  $\bar{\bar{G}}_{AJ}(\bar{\mathbf{k}}, \bar{\mathbf{r}}')$  as:

$$\bar{\bar{G}}_{AJ}(\bar{\mathbf{r}}, \bar{\mathbf{r}}') = \frac{1}{(2\pi)^3} \iiint_{-\infty}^{+\infty} \frac{\bar{\bar{Z}}_A^a}{|\bar{\bar{Z}}_A|} e^{-j\bar{\mathbf{k}} \cdot (\bar{\mathbf{r}} - \bar{\mathbf{r}}')} d\bar{\mathbf{k}}. \quad (17)$$

Actually, from Equations (8) and (10), we can obtain the expression of  $\mathbf{E}$  in term of  $\mathbf{A}$  in the spatial domain as:

$$\mathbf{E} = -j\omega\mathbf{A} - \frac{j}{\omega\mu_z\epsilon_z^2} \nabla\nabla \cdot \bar{\bar{\epsilon}}\mathbf{A}. \quad (18)$$

Therefore, if  $\mathbf{E}$  and  $\mathbf{A}$  in Equation (18) are excited by the same unit point source, the DGF  $\bar{\bar{G}}_{EJ}(\bar{\mathbf{k}}, \bar{\mathbf{r}}')$  of electric field and the DGFA  $\bar{\bar{G}}_{AJ}(\bar{\mathbf{k}}, \bar{\mathbf{r}}')$  in the spectral domain can be related by:

$$\bar{\bar{G}}_{EJ}(\bar{\mathbf{k}}, \bar{\mathbf{r}}') = -j\omega \left( \bar{\mathbf{I}} - \frac{1}{\omega^2\mu_z\epsilon_z^2} \begin{bmatrix} k_x^2\epsilon_x & k_xk_y\epsilon_x & k_xk_z\epsilon_z \\ k_xk_y\epsilon_x & k_y^2\epsilon_x & k_yk_z\epsilon_z \\ k_xk_z\epsilon_x & k_yk_z\epsilon_x & k_z^2\epsilon_z \end{bmatrix} \right) \bar{\bar{G}}_{AJ}(\bar{\mathbf{k}}, \bar{\mathbf{r}}'). \quad (19)$$

Substituting (15) into (19), we obtain the spectral domain DGF of electric field as:

$$\bar{\bar{W}}_E \bar{\bar{G}}_{EJ}(\bar{\mathbf{k}}, \bar{\mathbf{r}}') = j\omega e^{j\bar{\mathbf{k}} \cdot \bar{\mathbf{r}}'}, \quad (20)$$

where  $\bar{\bar{W}}_E$  is electric wave matrix and its detailed expression is shown in the Appendix C.

Equation (20) is in accord with the results shown in the paper [20], [24].

### III. EVALUATION

The spatial DGFA  $\bar{\bar{G}}_{AJ}$  in Equation (17) is not easy to compute due to its triple integral. It is noted, however, that  $\bar{\bar{Z}}_A$  is a sixth order polynomial of  $k_z$ , and thus, has six different roots. So it can be written as:

$$|\bar{\bar{Z}}_A| = \alpha_6 \prod_{i=1}^3 (k_z - k_{z,i}^u)(k_z - k_{z,i}^d), \quad (21)$$

where the subscript  $i = (1,2,3)$ . The wave vectors  $k_{z,i}^u$  and  $k_{z,i}^d$  are couple positive and negative roots corresponding to upward and downward propagating

wave, respectively. Let's define  $k_\rho = \sqrt{k_x^2 + k_y^2}$ , so  $k_{z,i}^u$  and  $k_{z,i}^d$  depend only on  $k_\rho$ . The coefficient  $\alpha_6 = \frac{1}{\mu_x^2\mu_z}$ .

Substituting (21) into (17), we obtain the spatial domain DGFA as:

$$\bar{\bar{G}}_{AJ}(\bar{\mathbf{r}}, \bar{\mathbf{r}}') = \frac{1}{(2\pi)^3} \iiint_{-\infty}^{+\infty} \frac{\bar{\bar{Z}}_A^a(k_z)}{\alpha_6 \prod_{i=1}^3 (k_z - k_{z,i}^u)(k_z - k_{z,i}^d)} e^{-j\bar{\mathbf{k}} \cdot (\bar{\mathbf{r}} - \bar{\mathbf{r}}')} d\bar{\mathbf{k}}. \quad (22)$$

In order to avoid singularities in the evaluation of  $\bar{\bar{G}}_{AJ}$ , we apply the Cauchy residue theorem to (22). The triple integral of  $\bar{\bar{G}}_{AJ}$  is reduced to a double integral as:

$$\bar{\bar{G}}_{AJ}(\bar{\mathbf{r}}, \bar{\mathbf{r}}') = \frac{j}{(2\pi)^2} \sum_{i=1}^3 \begin{cases} \iint_{-\infty}^{+\infty} \frac{\bar{\bar{Z}}_A^a(k_{z,i}^u)}{\det \bar{\bar{Z}}_A(k_{z,i}^u)} e^{-j\bar{\mathbf{k}}_i^u \cdot (\bar{\mathbf{r}} - \bar{\mathbf{r}}')} dk_x dk_y, z \geq z' \\ \iint_{-\infty}^{+\infty} \frac{\bar{\bar{Z}}_A^a(k_{z,i}^d)}{\det \bar{\bar{Z}}_A(k_{z,i}^d)} e^{-j\bar{\mathbf{k}}_i^d \cdot (\bar{\mathbf{r}} - \bar{\mathbf{r}}')} dk_x dk_y, z \leq z' \end{cases}, \quad (23)$$

where the subscript  $i = (1,2,3)$  is a cyclic index with a period of 3, and  $h = (u, d)$  for:

$$\bar{\mathbf{k}}_i^h = \hat{\mathbf{x}}k_x + \hat{\mathbf{y}}k_y + \hat{\mathbf{z}}k_{z,i}^h, \quad (24)$$

$$\det \bar{\bar{Z}}_A(k_{z,i}^h) = 2\alpha_6 k_{z,i}^h \sum_{m=1}^2 (|k_{z,i}^h|^2 - |k_{z,i+m}^h|^2). \quad (25)$$

$k_{z,i}^u$  and  $k_{z,i}^d$  are couple positive and negative roots, so it's easily verified that there are the same result for any two points with the symmetry of  $(x', y')$  plane in Equation (23). So here we only derive the DGFA for  $z \geq z'$ . Let

$$\bar{\bar{G}}_A(k_{z,i}^u) = \frac{\bar{\bar{Z}}_A^a(k_{z,i}^u)}{\det \bar{\bar{Z}}_A(k_{z,i}^u)}, \quad (26)$$

and by simplifying Equation (26), we obtain  $i = (1,2)$  for:

$$\bar{\bar{G}}_A(k_{z,i}^u) = \begin{bmatrix} g_{i,1}(k_\rho)k_x^2 & g_{i,2}(k_\rho)k_xk_y & g_{i,3}(k_\rho)k_x \\ g_{i,2}(k_\rho)k_xk_y & g_{i,4}(k_\rho)k_y^2 & g_{i,5}(k_\rho)k_y \\ g_{i,3}(k_\rho)k_x & g_{i,5}(k_\rho)k_y & g_{i,6}(k_\rho) \end{bmatrix}, \quad (27)$$

and  $i = 3$  for:

$$\bar{\bar{G}}_A(k_{z,3}^u) = \begin{bmatrix} g_{3,1}(k_\rho)k_x^2 & g_{3,2}(k_\rho)k_xk_y & 0 \\ g_{3,2}(k_\rho)k_xk_y & g_{3,3}(k_\rho)k_y^2 & 0 \\ 0 & 0 & 0 \end{bmatrix}, \quad (28)$$

where  $g_{i,j}(k_\rho)$  is the function of  $k_\rho$ ,  $i = (1,2,3)$ ,  $j = (1,2,3,4,5,6)$ .

Substituting (27) and (28) into (23), we can see that each term in Equation (23) for  $z \geq z'$  is reduced to a Sommerfeld integral [33] as:

$$\mathbf{G}_{AJ}^{(i,j)} = \frac{1}{2\pi} F_{i,j}(\epsilon, \mu, \rho, \varphi) \int_0^{+\infty} f_{i,j}(k_{z,i}^u | k_\rho) J_n(k_\rho \rho) k_\rho^m dk_\rho, \quad (29)$$

where  $F_{i,j}(\epsilon, \mu, \rho, \varphi)$  is the coefficient expression of  $(\epsilon, \mu, \rho, \varphi)$ ,  $\epsilon = (\epsilon_x, \epsilon_z)$ ,  $\mu = (\mu_x, \mu_z)$ ,  $m = (0,1,2,3)$ .  $(\rho, \varphi)$  are the cylindrical coordinates of the projection of the source point on the  $(x, y)$  plane, and  $\rho =$

$\sqrt{(x-x')^2 + (y-y')^2}$ .  $J_n$  is the Bessel function of order  $n = (0,1)$ .  $f_{i,j}(k_{z,i}^u | k_\rho)$  is the function of  $k_{z,i}^u$  which is expressed by  $k_\rho$ , and it shows as (30) for  $l = (-1,0,1)$ :

$$f_{i,j}(k_{z,i}^u | k_\rho) = (k_{z,i}^u)^l e^{-jk_{z,i}^u(z-z')}. \quad (30)$$

So the spatial domain DGFA is a symmetric matrix, and it can be written as:

$$\bar{\mathbf{G}}_{\mathbf{AJ}}(\bar{\mathbf{r}}, \bar{\mathbf{r}}') = \begin{bmatrix} G_{11} & G_{12} & G_{13} \\ G_{12} & G_{22} & G_{23} \\ G_{13} & G_{23} & G_{33} \end{bmatrix}, \quad (31)$$

where

$$G_{11} = \mathbf{G}_{\mathbf{AJ}}^{(1,1)} + \mathbf{G}_{\mathbf{AJ}}^{(2,1)} + \mathbf{G}_{\mathbf{AJ}}^{(3,1)}, \quad (32)$$

$$G_{12} = \mathbf{G}_{\mathbf{AJ}}^{(1,2)} + \mathbf{G}_{\mathbf{AJ}}^{(2,2)} + \mathbf{G}_{\mathbf{AJ}}^{(3,2)}, \quad (33)$$

$$G_{13} = \mathbf{G}_{\mathbf{AJ}}^{(1,3)} + \mathbf{G}_{\mathbf{AJ}}^{(2,3)}, \quad (34)$$

$$G_{22} = \mathbf{G}_{\mathbf{AJ}}^{(1,4)} + \mathbf{G}_{\mathbf{AJ}}^{(2,4)} + \mathbf{G}_{\mathbf{AJ}}^{(3,3)}, \quad (35)$$

$$G_{23} = \mathbf{G}_{\mathbf{AJ}}^{(1,5)} + \mathbf{G}_{\mathbf{AJ}}^{(2,5)}, \quad (36)$$

$$G_{33} = \mathbf{G}_{\mathbf{AJ}}^{(1,6)} + \mathbf{G}_{\mathbf{AJ}}^{(2,6)}. \quad (37)$$

Because the Sommerfeld integrands of (29) have slow decaying and intensive oscillation, straightforward numerical integration methods are not efficient. In order to reach an accurate but efficient evaluation of (29), we need to change the integrands by the singularity subtraction method [31]. In this way, an equation with the same decaying and oscillation of Equation (29) was designed as:

$$M_{(i,j)}(k_{\rho,i}^*) = \int_0^{+\infty} f_{i,j}^*(k_{\rho,i}^*) J_n(k_{\rho,i}^* \rho_i^*) k_{\rho,i}^m dk_{\rho,i}^*, \quad (38)$$

where  $k_{\rho,i}^*$  is the asymptotic form of  $k_{z,i}^u$ , and

$$\lim_{k_\rho \rightarrow \infty} k_{z,i}^u \approx jQ_i(\epsilon, \mu) k_\rho = jk_{\rho,i}^*, \quad (39)$$

$$\rho_i^* = \frac{\rho}{Q_i(\epsilon, \mu)}, \quad (40)$$

$Q_i(\epsilon, \mu)$  is the coefficient expression of  $(\epsilon, \mu)$ ,  $\epsilon = (\epsilon_x, \epsilon_z)$ ,  $\mu = (\mu_x, \mu_z)$ . And there is an analytical solution for  $M_{i,j}(k_{\rho,i}^*)$  by the following identity [35]:

$$\int_0^{+\infty} e^{-k_\rho \alpha} J_n(k_\rho \rho) k_\rho^m dk_\rho = (-1)^m \rho^{-n} \frac{d^m}{d\alpha^m} \left[ \frac{(\sqrt{\rho^2 + \alpha^2} - \alpha)^n}{\sqrt{\rho^2 + \alpha^2}} \right], \quad (41)$$

where  $\rho > 0$ ,  $n > -m - 1$ .

With the subtraction  $M_{i,j}(k_{\rho,i}^*)$ , Equation (29) can be deformed as:

$$\mathbf{G}_{\mathbf{AJ}}^{(i,j)} = \mathbf{G}_{\mathbf{AJ}}^{(i,j)} - \tilde{\mathbf{G}}_{\mathbf{AJ}}^{(i,j)} + \tilde{\mathbf{G}}_{i,j}, \quad (42)$$

where  $\tilde{\mathbf{G}}_{i,j}$  is the analytical solution of  $\tilde{\mathbf{G}}_{\mathbf{AJ}}^{(i,j)}$ , and

$$\tilde{\mathbf{G}}_{\mathbf{AJ}}^{(i,j)} = \frac{1}{2\pi} F_{i,j}(\epsilon, \mu, \rho, \varphi) M_{(i,j)}(k_{\rho,i}^*). \quad (43)$$

If  $\rho = 0$ , there are singularities in Equation (29). So here we will discuss how to deal with this problem. As  $\rho$  approaches zero, the asymptotic behaviors of the cylindrical wave functions for  $k_\rho \rho \rightarrow 0$  are:

$$J_0(k_\rho \rho) \sim 1, \quad (44)$$

$$J_0(k_\rho \rho) \sim \frac{k_\rho \rho}{2}. \quad (45)$$

Substituting (44) and (45) into (29), we can easily obtain the DGFA for  $\rho \rightarrow 0$  as:

$$\bar{\mathbf{G}}_{\mathbf{AJ}}(\bar{\mathbf{r}}, \bar{\mathbf{r}}') = \begin{bmatrix} G_{11} & 0 & G_{13} \\ 0 & G_{22} & G_{23} \\ G_{13} & G_{23} & G_{33} \end{bmatrix}, \quad (46)$$

where

$$G_{11} = G_{22} = \int_0^{+\infty} C_1 k_{z,1}^u e^{-jk_{z,1}^u(z-z')} k_\rho + C_2 \frac{e^{-jk_{z,2}^u(z-z')}}{k_{z,2}^u} k_\rho^3 + C_3 \frac{e^{-jk_{z,3}^u(z-z')}}{k_{z,3}^u} k_\rho dk_\rho, \quad (47)$$

$$G_{13} = G_{31} = C_4(x-x') \int_0^{+\infty} k_\rho^3 (e^{-jk_{z,1}^u(z-z')} - e^{-jk_{z,2}^u(z-z')}) dk_\rho, \quad (48)$$

$$G_{23} = G_{32} = C_5(y-y') \int_0^{+\infty} k_\rho^3 (e^{-jk_{z,1}^u(z-z')} - e^{-jk_{z,2}^u(z-z')}) dk_\rho, \quad (49)$$

$$G_{33} = \int_0^{+\infty} C_6 \frac{e^{-jk_{z,1}^u(z-z')}}{k_{z,1}^u} k_\rho^3 + C_7 k_{z,2}^u e^{-jk_{z,2}^u(z-z')} k_\rho dk_\rho, \quad (50)$$

$C_i$ ,  $i = [1,2,3,4,5,6,7]$ , is the coefficient expression of  $(\epsilon, \mu)$ ,  $\epsilon = (\epsilon_x, \epsilon_z)$ ,  $\mu = (\mu_x, \mu_z)$ .

When  $z = z'$ , it is easily verified that  $G_{11} = G_{22} = \infty$ ,  $G_{33} = \infty$ ,  $G_{13} = G_{31} = 0$  and  $G_{23} = G_{32} = 0$ . In this way, the DGFA becomes a diagonal dyad.

#### IV. NUMERICAL VALIDATION

The aforementioned derivations indicate the solution process of DGFA. However, it is difficult to verify the solutions because most commercial numerical simulation software computes field intensity  $\mathbf{E}$  and  $\mathbf{H}$  instead of magnetic vector potential  $\mathbf{A}$ . Therefore, in this work, we verified our derivations for the DGFA in three steps. First, we calculated the  $\bar{\mathbf{G}}_{\mathbf{AJ}}$  for a degenerated case, i.e., for the unbounded isotropic medium since there was an analytical solution for  $\bar{\mathbf{G}}_{\mathbf{AJ}}$  in the isotropic media. In the second step, by using (18), also in the circumstance of an isotropic medium, we computed  $\mathbf{E}$  from  $\mathbf{A}$  which is assumed to be generated by an infinitesimal electric dipole source. We compared these calculated  $\mathbf{E}$  field values to the results simulated by the commercial software COMSOL. Finally, following the similar procedure, we compared  $\mathbf{E}$  field values computed from  $\bar{\mathbf{G}}_{\mathbf{AJ}}$  and those from COMSOL simulations but for uniaxial anisotropic media.

In the unbounded homogeneous isotropic space, the DGFA becomes an analytical scalar instead of a dyad. And it is expressed as:

$$g(\bar{\mathbf{r}}, \bar{\mathbf{r}}') = \mu \frac{e^{-jk|\bar{\mathbf{r}}-\bar{\mathbf{r}}'|}}{4\pi|\bar{\mathbf{r}}-\bar{\mathbf{r}}'|}. \quad (51)$$

In the computation, for case 1, we set that the permeability  $\mu = 10\mu_0$ , the permittivity  $\epsilon = 10\epsilon_0$ , and electric conductivity  $\sigma = 0.0001\text{S/m}$ , where  $\mu_0$  and  $\epsilon_0$  are the permeability and permittivity in the free space. We choose a computation domain of  $6\text{ m} \times 6\text{ m} \times 6\text{ m}$ , where 216 observation points are uniformly distributed. The electric dipole source is located in the center of the region, and the operation frequency is 1 GHz. The  $\bar{\mathbf{G}}_{\mathbf{AJ}}$  dyadics of those 216 points evaluated by the Sommerfeld integrals in Equation (42) only show non-

zero diagonal values while having zero values in all the off-diagonal elements. Figure 1 shows the good agreements between DGFA computation and the analytical solutions for those non-zero diagonal elements. Only 72 of 216 points (sampled uniformly per three points) are shown to make the comparisons more discernable.

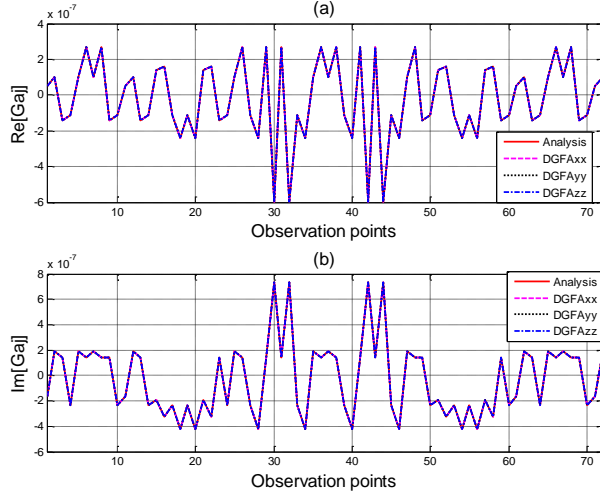


Fig. 1. Comparisons of the diagonal values of  $\bar{\mathbf{G}}_{\mathbf{A}\mathbf{J}}$  and the analytical solutions: (a) depicts the real part, and (b) depicts the imaginary part.

We define the relative error as:

$$Err_{ii} = \sqrt{\frac{\|g - [\bar{\mathbf{G}}_{\mathbf{A}\mathbf{J}}]_{ii}\|^2}{\|g\|^2}}, \quad (52)$$

where  $\| \cdot \|$  is L2 norm and  $ii = (xx, yy, zz)$ . Using this definition, we calculated the relative numerical error for the evaluation of  $\bar{\mathbf{G}}_{\mathbf{A}\mathbf{J}}$  and found that  $Err_{xx} = 3.0772 \times 10^{-7}$ ,  $Err_{yy} = 3.0772 \times 10^{-7}$ , and  $Err_{zz} = 3.0650 \times 10^{-7}$ .

In order to save computation of resource for COMSOL simulation of electromagnetic wave propagating inside a homogeneous isotropic medium, we decreased the computation domain to  $0.3 \text{ m} \times 0.3 \text{ m} \times 0.3 \text{ m}$ . We performed the simulations for two cases. In case 2, we set  $\mu = \mu_0$ ,  $\varepsilon = \varepsilon_0$  and  $\sigma = 0.0001 \text{ S/m}$ . In case 3, we set  $\mu = 0.1\mu_0$ ,  $\varepsilon = 0.1\varepsilon_0$  and  $\sigma = 0.0001 \text{ S/m}$ . The 216 observation points are also uniformly distributed within the domain. The electric dipole polarized by (1,1,1) is located in the center of the region and radiates 1 GHz electromagnetic waves. In the COMSOL simulation models, the source location as well as its polarization and the electrical parameters such as  $\mu$ ,  $\varepsilon$  and  $\sigma$  are the same as those used in the DGFA computation. The mesh sizes are set to be 'EXTRA FINE' and the thickness of the perfect match layers (PML) is set as 0.15 m which are located outside the computation domain. The mesh sizes and PML thickness are the same for all the COMOSL

simulations presented in this paper. When we computed  $\mathbf{E}$  from  $\mathbf{A}$  using (18), numerical central differential method was applied to gradient and divergence operation.

The comparisons for the electric fields among analytic solutions, calculations from DGFA  $\bar{\mathbf{G}}_{\mathbf{A}\mathbf{J}}$  and simulations by COMSOL are shown in Fig. 2. Here, only 54 (sampled uniformly per four points) representative points of 216 are chosen to make the comparisons more discernable. Moreover, we only show the  $x$ -component comparisons for case 2 while  $y$ -component comparisons for case 3. Comparisons for other components are not presented since they are similar as those for the  $x$ -component or the  $y$ -component. In order to evaluate the computation error, we give an error definition similar as (52):

$$Err_i = \sqrt{\frac{\|E_{ana} - E_i\|^2}{\|E_{ana}\|^2}}, \quad (53)$$

where  $i = (COMSOL, DGFA)$  and  $E_{ana}$  is the analytical solution calculated using (51).

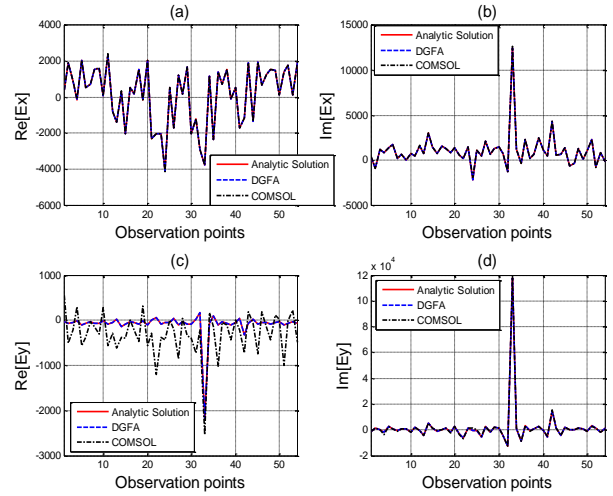


Fig. 2. Comparisons of electric fields computed by analytical methods, using DGFA and from COMSOL simulations in an isotropic medium: (a) and (b) are for case 2; (c) and (d) are for case 3; (a) and (c) depict the real parts while (b) and (d) depict the imaginary parts.

Figures 2 (a) and (b) show the comparisons of  $E_x$  in case 2. The relative error between calculations using DGFA and the analytical solutions is  $9.441 \times 10^{-8}$ . The relative error between COMSOL simulations and the analytical solutions is  $9.9 \times 10^{-3}$ . We can see that the  $x$ -components of  $\mathbf{E}$  computed in three ways show good agreements. Figures 2 (c) and (d) show the comparisons of  $E_y$  in case 3. The relative error between calculations using DGFA and the analytical solutions is  $1.2608 \times 10^{-7}$ . The relative error between COMSOL simulations and the analytical solutions is  $3.14 \times 10^{-2}$ . There is an obvious mismatch between COMSOL simulations and

analytical solutions in Fig. 2 (c). Actually, not only the  $E_y$  real part has this mismatch, but also the real part of  $E_x$  and  $E_z$  which are not shown here. This mismatch may be due to that the imaginary part is around 50 times larger than the real part and thus the numerical iteration precision cannot be maintained for the real parts which have much smaller values.

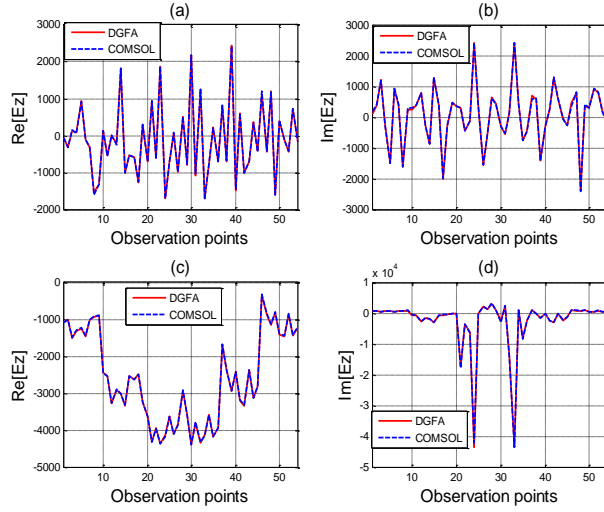


Fig. 3. Comparisons of electric fields computed using DGFA and from COMSOL simulations in an uniaxial anisotropic medium: (a) and (b) are for case 4; (c) and (d) are for case 5; (a) and (c) depict the real parts while (b) and (d) depict the imaginary parts.

In aforementioned two steps, we verified the derivation of  $\bar{\mathbf{G}}_{AJ}$  in the circumstance of isotropic media. Now let us check its correctness inside a uniaxial anisotropic media. Since there is no analytical solution for the  $\mathbf{E}$  field in uniaxial anisotropic media, we only compare the electric fields computed using  $\bar{\mathbf{G}}_{AJ}$  and simulated by COMSOL. The simulation domain, observation points, the source dipole position as well as its polarization are the same as in previous case 2 and case 3. However, we use following dielectric parameters in case 4:

$$\bar{\boldsymbol{\mu}} = \mu_0 \begin{bmatrix} 1 & 0 & 0 \\ 0 & 1 & 0 \\ 0 & 0 & 5 \end{bmatrix}, \quad \bar{\boldsymbol{\varepsilon}} = \varepsilon_0 \begin{bmatrix} 1 & 0 & 0 \\ 0 & 1 & 0 \\ 0 & 0 & 5 \end{bmatrix},$$

$$\bar{\boldsymbol{\sigma}} = \begin{bmatrix} 0.001 & 0 & 0 \\ 0 & 0.001 & 0 \\ 0 & 0 & 0.005 \end{bmatrix} \text{ S/m.} \quad (54)$$

And we use following dielectric parameters in case 5:

$$\bar{\boldsymbol{\mu}} = \mu_0 \begin{bmatrix} 1 & 0 & 0 \\ 0 & 1 & 0 \\ 0 & 0 & 0.1 \end{bmatrix}, \quad \bar{\boldsymbol{\varepsilon}} = \varepsilon_0 \begin{bmatrix} 1 & 0 & 0 \\ 0 & 1 & 0 \\ 0 & 0 & 0.1 \end{bmatrix},$$

$$\bar{\boldsymbol{\sigma}} = \begin{bmatrix} 0.001 & 0 & 0 \\ 0 & 0.001 & 0 \\ 0 & 0 & 0.0001 \end{bmatrix} \text{ S/m.} \quad (55)$$

Figure 3 shows the comparisons of  $z$ -component of  $\mathbf{E}$  between calculations using DGFA and simulations by COMSOL. Here, we also choose 54 representative points. We can see that  $E_z$  values are highly consistent for two computation methods for both real parts and imaginary parts in two cases. If the relative error between these two results is defined as:

$$Err_{CD} = \sqrt{\frac{\|E_{DGFA} - E_{COMSOL}\|^2}{\|E_{DGFA}\|^2}}. \quad (56)$$

The error for case 4 is  $2.32 \times 10^{-2}$ , and,  $3.33 \times 10^{-2}$  for case 5.

In our work, we use the singularity subtraction method [31] to accelerate the integral process of Equation (29), which is calculated segment by segment on the Sommerfeld integral path until the desired accuracy is obtained [31]. If the efficiency improvement is defined as:

$$Effi = \frac{ISN_{wo} - ISN_w}{ISN_{wo}}, \quad (57)$$

where  $ISN$  is the number of the segments for the Sommerfeld integrals, and subscript  $wo/w$  means without/with subtraction.

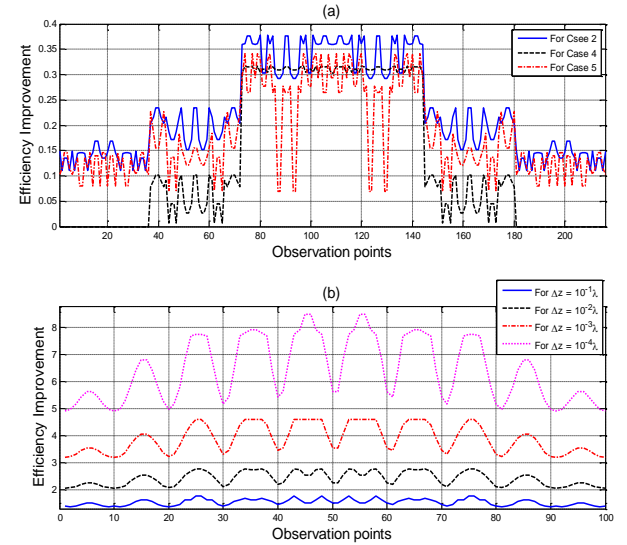


Fig. 4. Efficiency improvements for different cases through the singularity subtraction method: (a) is for case 2, case 4 and case 5; (b) is for extreme cases in which observation points get closer to the  $z'$  plane.

Figure 4 shows the efficiency improvements by the subtraction method. Figure 4 (a) displays the results for case 2, case 4 and case 5. It is clear that the efficiency improvements are different for different observation points. When the observation points are far from the source point in the  $z$  direction, i.e., when  $|z - z'|$  values are large, the efficiency improvements are not obvious. However, when  $|z - z'|$  becomes smaller, efficiency improvements become obvious, and reach about 30%

in case 2, case 4 and case 5. We further decrease the distance in the  $z$  direction between the source point and field points to verify the efficiency improvement. Figure 4 (b) shows the results for  $\Delta z = |z - z'|$  of  $10^{-1}\lambda$ ,  $10^{-2}\lambda$ ,  $10^{-3}\lambda$  and  $10^{-4}\lambda$ . All the computation is performed in the same background medium with dielectric parameter shown in (54). And 100 observation points are uniformly distributed in the computation domain. Clearly, after the subtraction, the smaller is  $\Delta z$ , the larger is the efficiency improvement. If the observation points are placed in the source plane, i.e.,  $|z - z'| = 0$ , it is easy to verify that Equation (29) can't converge, but Equation (42) can converge with very few number of the integral segments under the desired accuracy. Therefore, the efficiency improvement by the singularity subtraction method becomes more significant when the observation points get closer to the source point in the  $z$  direction.

## V. SUMMARY AND CONCLUSIONS

In this paper, the DGFA formula for the unbounded uniaxial anisotropic media were derived. Starting from Maxwell's equations and through the forward and inverse spatial Fourier transforms, DGFA formula in the integral forms were obtained for three-dimensional cases. Based upon Cauchy residue theorem, the closed form of DGFA formula were finally simplified to one-dimensional Sommerfeld integrals. By applying the singularity subtraction method and Gaussian quadrature, we can efficiently and accurately evaluate these Sommerfeld integrals. The numerical accuracy was only restricted by the Gaussian quadrature. In an effort to verify our derivations for those formula, we compared our results with analytical and simulated results in the circumstance of isotropic and uniaxial anisotropic media respectively. These comparisons showed that the results obtained from the DGFA and those by analytical methods and numerical simulations agreed well. The effect of the singularity subtraction was validated by several numerical experiments. Hence, the derivation and evaluation of DGFA presented in this paper are reliable and efficient.

## ACKNOWLEDGMENT

This work was supported by the National Natural Science Foundation of China under Grant No. 41504120, and the Education Department of Fujian Province, China under Grant No. JA14005.

## APPENDIX A. EXPRESSIONS OF $\bar{\bar{Z}}_E$

$$\bar{\bar{Z}}_E = \begin{bmatrix} Z_{E,11} & Z_{E,12} & Z_{E,13} \\ Z_{E,21} & Z_{E,22} & Z_{E,23} \\ Z_{E,31} & Z_{E,32} & Z_{E,33} \end{bmatrix}, \quad (\text{A1})$$

where:

$$Z_{E,11} = \frac{\varepsilon_x^2}{\mu_z \varepsilon_z^2} \frac{\partial^2}{\partial x^2} + \frac{1}{\mu_z} \frac{\partial^2}{\partial y^2} + \frac{1}{\mu_x} \frac{\partial^2}{\partial z^2} + \omega^2 \varepsilon_x, \quad (\text{A2})$$

$$Z_{E,12} = -\frac{1}{\mu_z} \frac{\partial^2}{\partial x \partial y} + \frac{\varepsilon_x^2}{\mu_z \varepsilon_z^2} \frac{\partial^2}{\partial x \partial y}, \quad (\text{A3})$$

$$Z_{E,13} = -\frac{1}{\mu_x} \frac{\partial^2}{\partial x \partial z} + \frac{\varepsilon_x}{\mu_z \varepsilon_z} \frac{\partial^2}{\partial x \partial z}, \quad (\text{A4})$$

$$Z_{E,21} = Z_{E,12}, \quad (\text{A5})$$

$$Z_{E,22} = \frac{1}{\mu_z} \frac{\partial^2}{\partial x^2} + \frac{\varepsilon_x^2}{\mu_z \varepsilon_z^2} \frac{\partial^2}{\partial y^2} + \frac{1}{\mu_x} \frac{\partial^2}{\partial z^2} + \omega^2 \varepsilon_x, \quad (\text{A6})$$

$$Z_{E,23} = -\frac{1}{\mu_x} \frac{\partial^2}{\partial y \partial z} + \frac{\varepsilon_x}{\mu_z \varepsilon_z} \frac{\partial^2}{\partial y \partial z}, \quad (\text{A7})$$

$$Z_{E,31} = Z_{E,13}, \quad (\text{A8})$$

$$Z_{E,32} = Z_{E,23}, \quad (\text{A9})$$

$$Z_{E,33} = \frac{1}{\mu_x} \left( \frac{\partial^2}{\partial x^2} + \frac{\partial^2}{\partial y^2} \right) + \frac{1}{\mu_z} \frac{\partial^2}{\partial z^2} + \omega^2 \varepsilon_z. \quad (\text{A10})$$

## APPENDIX B. EXPRESSIONS OF $\bar{\bar{Z}}_A$

$$\bar{\bar{Z}}_A = \begin{bmatrix} Z_{A,11} & Z_{A,12} & Z_{A,13} \\ Z_{A,21} & Z_{A,22} & Z_{A,23} \\ Z_{A,31} & Z_{A,32} & Z_{A,33} \end{bmatrix}, \quad (\text{B1})$$

where:

$$Z_{A,11} = \omega^2 \varepsilon_x - \frac{k_x^2 \varepsilon_x^2}{\mu_z \varepsilon_z^2} - \frac{k_y^2}{\mu_z} - \frac{k_z^2}{\mu_x}, \quad (\text{B2})$$

$$Z_{A,12} = \left( \frac{1}{\mu_z} - \frac{\varepsilon_x^2}{\mu_z \varepsilon_z^2} \right) k_x k_y, \quad (\text{B3})$$

$$Z_{A,13} = \left( \frac{1}{\mu_x} - \frac{\varepsilon_x}{\mu_z \varepsilon_z} \right) k_x k_z, \quad (\text{B4})$$

$$Z_{A,21} = Z_{A,12}, \quad (\text{B5})$$

$$Z_{A,22} = \omega^2 \varepsilon_x - \frac{k_x^2}{\mu_z} - \frac{k_y^2 \varepsilon_x^2}{\varepsilon_z^2 \mu_z} - \frac{k_z^2}{\mu_x}, \quad (\text{B6})$$

$$Z_{A,23} = \left( \frac{1}{\mu_x} - \frac{\varepsilon_x}{\mu_z \varepsilon_z} \right) k_y k_z, \quad (\text{B7})$$

$$Z_{A,31} = Z_{A,13}, \quad (\text{B8})$$

$$Z_{A,32} = Z_{A,23}, \quad (\text{B9})$$

$$Z_{A,33} = \omega^2 \varepsilon_z - \frac{k_x^2}{\mu_x} - \frac{k_y^2}{\mu_x} - \frac{k_z^2}{\mu_z}. \quad (\text{B10})$$

## APPENDIX C. EXPRESSIONS OF $\bar{\bar{W}}_A$

$$\bar{\bar{W}}_E = \begin{bmatrix} W_{E,11} & W_{E,12} & W_{E,13} \\ W_{E,21} & W_{E,22} & W_{E,23} \\ W_{E,31} & W_{E,32} & W_{E,33} \end{bmatrix}, \quad (\text{C1})$$

where:

$$W_{E,11} = \omega^2 \varepsilon_x - \frac{k_y^2}{\mu_z} - \frac{k_z^2}{\mu_x}, \quad (\text{C2})$$

$$W_{E,12} = \frac{k_x k_y}{\mu_z}, \quad (\text{C3})$$

$$W_{E,13} = \frac{k_x k_z}{\mu_x}, \quad (\text{C4})$$

$$W_{E,21} = W_{E,12}, \quad (\text{C5})$$

$$W_{E,22} = \omega^2 \varepsilon_x - \frac{k_x^2}{\mu_z} - \frac{k_z^2}{\mu_x}, \quad (\text{C6})$$

$$W_{E,23} = \frac{k_y k_z}{\mu_x}, \quad (\text{C7})$$

$$W_{E,31} = W_{E,13}, \quad (\text{C8})$$

$$W_{E,32} = W_{E,23}, \quad (\text{C9})$$

$$W_{E,33} = \omega^2 \varepsilon_z - \frac{k_x^2}{\mu_x} - \frac{k_y^2}{\mu_x}. \quad (\text{C10})$$

## REFERENCES

- [1] M. J. Havrilla, "Scalar potential depolarizing dyad

- artifact for a uniaxial medium,” *Progress In Electromagnetics Research*, vol. 134, no. 1, pp. 151-168, 2013.
- [2] M. J. Havrilla, “Scalar potential formulation for a uniaxial inhomogeneous medium,” *Radio Science Meeting (USNC-URSI NRSM)*, 2014.
- [3] W. S. Weiglhofer and S. O. Hansen, “Faraday chiral media revisited. I. Fields and sources,” *IEEE Transactions on Antennas and Propagation*, vol. 47, no. 5, pp. 807-814, 1999.
- [4] A. Y. Qing, “Electromagnetic inverse scattering of multiple perfectly conducting cylinders by differential evolution strategy with individuals in groups (GDES),” *IEEE Transactions on Antennas and Propagation*, vol. 52, no. 5, pp. 1223-1229, 2004.
- [5] L. P. Zha, R. S. Chen, and T. Su, “Fast EM scattering analysis for the hard targets in a layered medium by using the hierarchical vector basis functions,” *Applied Computational Electromagnetics Society Journal*, vol. 30, no. 11, pp. 1154-1160, 2015.
- [6] J. L. Hu, Z. P. Wu, H. Mccann, L. E. Davis, and C. G. Xie, “Sequential quadratic programming method for solution of electromagnetic inverse problems,” *IEEE Transactions on Antennas and Propagation*, vol. 53, no. 8, pp. 2680-2687, 2005.
- [7] D. W. Winters, B. D. Van Veen, and S. C. Hagness, “A sparsity regularization approach to the electromagnetic inverse scattering problem,” *IEEE Transactions on Antennas and Propagation*, vol. 58, no. 1, pp. 145-154, 2010.
- [8] X. M. Xu and Q. H. Liu, “The BCGS-FFT method for electromagnetic scattering from inhomogeneous objects in a planarly layered medium,” *IEEE Antennas and Wireless Propagation Letters*, vol. 1, no. 1, pp. 77-80, 2002.
- [9] F. H. Li, L. P. Song, and Q. H. Liu, “Three-dimensional reconstruction of objects buried in layered media using born and distorted born iterative methods,” *IEEE Antennas and Wireless Propagation Letters*, vol. 1, no. 2, pp. 107-111, 2004.
- [10] M. Pastorino, M. Raffetto, and A. Randazzo, “Electromagnetic inverse scattering of axially moving cylindrical targets,” *IEEE Transactions on Geoscience and Remote Sensing*, vol. 53, no. 3, pp. 1452-1462, 2015.
- [11] J. G. Wang, Z. Q. Zhao, Z. P. Nie, and Q. H. Liu, “Electromagnetic inverse scattering series method for positioning three-dimensional targets in near-surface two-layer medium with unknown dielectric properties,” *IEEE Geoscience and Remote Sensing Letters*, vol. 12, no. 2, pp. 299-303, 2015.
- [12] J. L. Xiong and W. C. Chew, “A newly developed formulation suitable for matrix manipulation of layered medium Green’s functions,” *IEEE Transactions on Antennas and Propagation*, vol. 58, no. 3, pp. 868-875, 2010.
- [13] A. Yakovlev, S. Ortiz, et al., “Electric dyadic Green’s functions for modeling resonance and coupling effects in waveguide-based aperture-coupled patch arrays,” *Applied Computational Electromagnetics Society Journal*, vol. 17, no. 2, pp. 123-133, 2002.
- [14] P. M. Smith, “Dyadic Green’s functions for multi-layer SAW substrates,” *IEEE Transactions on Ultrasonics, Ferroelectrics, and Frequency Control*, vol. 48, no. 1, pp. 171-179, 1999.
- [15] G. W. Hanson, “Dyadic Green’s function for a multilayered planar medium-A dyadic eigenfunction approach,” *IEEE Transactions on Antennas and Propagation*, vol. 52, no. 12, pp. 3350-3356, 2004.
- [16] E. Simsek and Q. H. Liu, “Fast computation of dyadic Green’s function for layered media and its application in interconnect simulations,” *IEEE Transactions on Antennas and Propagation*, vol. 3, no. 3, pp. 2783, 2004.
- [17] K. A. Michalski and J. R. Mosig, “Multilayered media Green’s functions in integral equation formulations,” *IEEE Transactions on Antennas and Propagation*, vol. 45, no. 3, pp. 508-519, 1997.
- [18] P. G. Cottis, C. N. Vazouras, and C. Spyrou, “Green’s function for an unbounded biaxial medium in cylindrical coordinates,” *IEEE Transactions on Antennas and Propagation*, vol. 47, no. 1, pp. 195-276 199, 1999.
- [19] P. G. Cottis and G. D. Kondylis, “Properties of the dyadic Green’s function for an unbounded anisotropic medium,” *IEEE Transactions on Antennas and Propagation*, vol. 43, no. 2, pp. 154-279 161, 1995.
- [20] Y. Huang and J. K. Lee, “Dyadic green’s functions for unbounded and two-layered general anisotropic media,” *Progress In Electromagnetics Research B*, vol. 30, no. 30, pp. 27-46, 2011.
- [21] F. L. Mesa, R. Marques, and M. Horno, “A general algorithm for computing the bidimensional spectral Green’s dyad in multilayered complex bianisotropic media: The equivalent boundary method,” *IEEE Transactions on Microwave Theory and Techniques*, vol. 39, no. 9, pp. 1640-1649, 1991.
- [22] A. Eroglu, Y. H. Lee, and J. K. Lee, “Dyadic Green’s functions for multi-layered uniaxially anisotropic media with arbitrarily oriented optic axes,” *IET Microwaves, Antennas, Propagation*, vol. 5, no. 15, pp. 1779-1788, 2011.
- [23] P. P. Ding, C. W. Qiu, Z. Sad, and S. P. Yeo, “Rigorous derivation and fast solution of spatial domain Green’s functions for uniaxial anisotropic multilayers using modified fast Hankel transform

- method," *IEEE Transactions on Microwave Theory and Techniques*, vol. 60, no. 2, pp. 205-217, 2012.
- [24] S. M. Ali and S. F. Mahoud, "Electromagnetic fields of buried sources in stratified anisotropic media," *IEEE Transactions on Antennas and Propagation*, vol. 27, no. 5, pp. 671-678, 1979.
- [25] D. H. Werner, "An exact integration procedure for vector potentials of thin circular loop antennas," *IEEE Transactions on Antennas and Propagation*, vol. 44, no. 8, pp. 157-165, 1996.
- [26] N. Georgieva, Z. Z. Chen, and P. Bhartia, "Analysis of transient electromagnetic fields based on the vector potential function," *IEEE Transactions on Magnetics*, vol. 35, no. 3, pp. 1410-1413, 1999.
- [27] F. De. Flaviis, M. G. Noro, R. E. Diaz, G. Franceschetti, and N. G. Alexopoulos, "A time-domain vector potential formulation for the solution of electromagnetic problems," *IEEE Microwave and Guided Wave Letters*, vol. 8, no. 9, pp. 310-312, 1998.
- [28] Z. R. Yu, W. J. Zhang, and Q. H. Liu, "A mixed-order stabilized bi-conjugate gradient FFT method for magnetodielectric objects," *IEEE Transactions on Antennas and Propagation*, vol. 62, no. 11, pp. 5647-5655, 2014.
- [29] Z. R. Yu, W. J. Zhang, and Q. H. Liu, "The mixed-order BCGS-FFT method for the scattering of three-dimensional inhomogeneous anisotropic magnetodielectric objects," *IEEE Transactions on Antennas and Propagation*, vol. 63, no. 12, pp. 5709-5717, 2015.
- [30] R. D. Nevels and J. Jeong, "Time domain coupled field dyadic Green function solution for Maxwell's equations," *IEEE Transactions on Antennas and Propagation*, vol. 56, no. 8, pp. 2761-2764, 2008.
- [31] J. H. Moran and S. Gianzero, "Effects of formation anisotropy on resistivity-logging measurements," *Geophysics*, vol. 44, no. 7, pp. 1266-1286, 1979.
- [32] A. Abubakar and T. M. Habashy, "A closed-form expression of the electromagnetic tensor Green's functions for a homogeneous TI-anisotropic medium," *IEEE Geoscience and Remote Sensing Letters*, vol. 3, no. 4, pp. 447-451, 2006.
- [33] E. Simsek, Q. H. Liu, and B. J. Wei, "Singularity subtraction for evaluation of Green's functions for multilayer media," *IEEE Transactions on Microwave Theory and Techniques*, vol. 54, no. 1, pp. 216-225, 2006.
- [34] W. C. Chew, "Vector potential electromagnetics with generalized gauge for inhomogeneous media: Formulation," *Progress in Electromagnetics Research*, vol. 149, pp. 69-84, 2014.
- [35] A. Jeffrey and D. Zwillinger, *Table of Integrals, Series, and Products*. Elsevier, Burlington, 2007.



**Jianliang Zhuo** received the B.S. degree in Communication Engineering and Business Administration, and the M.S. degree in Communication and Information System from the University of Electronic Science and Technology of China, Chengdu, China, in 2007 and 2011. He is currently pursuing the Ph.D. degree at Xiamen University, Xiamen, China. His research interests include fast forward solvers in electromagnetics and inverse scattering methods for microelectronics and RF system



**Feng Han** received his B.S. degree in Electronic Science from Beijing Normal University and M.S. degree in Geophysics from Peking University, China, in 2003 and 2006, respectively. He received his Ph.D. in Electrical Engineering from Duke University, USA, in 2011. He is currently working as an Assistant Professor with the Institute of Electromagnetics and Acoustics, Xiamen University, China. His current research interests include ionosphere remote sensing by radio atmospherics, electromagnetic full wave inversion by integral equations, reverse time migration image, and the design of electromagnetic detection system.



**Na Liu** received the Ph.D. degree in Computational Mathematics from University of Chinese Academy of Sciences, Beijing, China, in 2013. From April 2012 to April 2013, she was a visiting student in the Department of Electrical and Computer Engineering, Duke University, Durham, NC. From November 2013 to January 2017, she was a Post-doctoral with Xiamen University where she is now an Associate Professor in Institute of Electromagnetics and Acoustics, Xiamen University, China. Her research is on computational electromagnetics, especially the fast and efficient methods for complex media and their applications in cavities, optical waveguide problems.



**Longfang Ye** received the Ph.D. degree in Electromagnetic Field and Microwave Technology from the University of Electronic Science and Technology of China, Chengdu, China, in 2013. From Oct. 2011 to Jan. 2013, he was a visiting student at Massachusetts Institute of Tech-

nology, Cambridge, MA, USA. Since July 2013, he has been an Assistant Professor with the Institute of Electromagnetics and Acoustics and Department of Electronic Science, Xiamen University, Xiamen, China. His current research interests include microwave circuits and antennas, terahertz waveguides and graphene-based devices.



**Hai Liu** received his B.E. and M.E. degrees in Civil Engineering from Tongji University, Shanghai, China, in 2007 and 2009, respectively. He received his Ph.D. in Environmental Studies from Tohoku University, Sendai, Japan in 2013. He is currently working as an Assistant

Professor with the Institute of Electromagnetics and Acoustics, Xiamen University, Xiamen, China. He was with the Center for Northeast Asian Studies at Tohoku University, Sendai, Japan as a Research Fellow from April 2013 to March 2014. His current research interests include the development of ground-penetrating radar systems and algorithms for a wide variety of applications, such as non-destructive testing in civil engineering, environmental monitoring, archeological investigation and lunar exploration.



**Qing Huo Liu** received his B.S. and M.S. degrees in Physics from Xiamen University, China in 1983 and 1986, and Ph.D. degree in Electrical Engineering from the University of Illinois at Urbana-Champaign in 1989. His research interests include computational electromagnetics and acoustics, inverse problems, and their applications in nanophotonics, geophysics, biomedical imaging, and electronic packaging. He has published over 400 papers in refereed journals and 500 papers in conference proceedings. He was with the Electromagnetics Laboratory at the University of Illinois at Urbana-Champaign as a Research Assistant from September 1986 to December 1988, and as a Postdoctoral Research Associate from January 1989 to February 1990. He was a Research Scientist and Program Leader with Schlumberger-Doll Research, Ridgefield, CT from 1990 to 1995. From 1996 to May 1999 he was an Associate Professor with New Mexico State University. Since June 1999 he has been with Duke University where he is now a Professor of Electrical and Computer Engineering. He received the 2017 ACES Technical Achievement Award.